

Identification of Unbalance and High Order Sensor Runout on Rigid Rotor Supported by Magnetic Bearings

Tea-Jin Park

Dept. of Intelligent Machinery and Systems, Graduate school, Kyushu University,
Hakozaki 6-10-1, Higashi-ku Fukuoka, 812-8581 Japan
tjpark@sky.mech.kyushu-u.ac.jp

Yoichi Kanemitsu, Kyushu University
Shinya Kijimoto, Kyushu University
Koichi Matsuda, Kyushu University
Yosuke Koba, Kyushu University

Abstract

In this paper, we have conducted identification experiments on the mass unbalance and high order sensor runout in a turbo molecular pump supported by active magnetic bearings (AMB), by using the proposed identification method. Firstly, output signals from the displacement sensors are converted and stored in the digital signal processor (DSP) board. The mass unbalance and high-order sensor runout are identified using the weighted-incremental least square on-line method from the stored displacement data. Next, by attaching known plural weights on the rotor, the resulting unbalance and higher-order sensor runout were identified using the proposed method. Finally, the reproducibility of the identification experiment and the effectiveness and accuracy of the proposed identification method were verified.

Introduction

The active magnetic bearing controls the electro magnetic force, which levitates and supports the rotor without physical contact. The mass unbalance in the rotor is caused by machining inaccuracy and assembling tolerance, which is the dominant cause of synchronous whirling of the rotor.

On the other hand, the eddy current type displacement sensor, which is used for measuring the gap between the levitated rotor and the stator of AMB, also detects electromagnetic ununiformity on the rotor surface and mechanical deformation of the circumferential surface of the rotor, which is called

sensor runout (SRO). The sensor runout is also a dominant factor causing the whirl of the rotor as well as the unbalance.

Thus, to date, numerous studies have been carried out on the measurement and compensation of the periodic whirl, which is synchronized with the rotor [1-3].

Recent studies on the issue have looked into adaptive feedforward control for the cancellation of periodic whirling and several researches have been conducted to coincide the mass center with the geometry center by observing the displacement and compensating the current signal[4-5].

In addition, other researches [5-6] have investigated robustness control that estimates and amends the sensor runout which is included in the whirling data of the rotor. Various studies [7-8] have also considered include repetitive and non-repetitive whirling to control the rotor without vibration.

However, none of the current research has carried out studies to identify the amplitude of the unbalance, higher-order SRO and phases at the same time. Setiawan, Mukherjee and Maslen [9] dealt with adaptive control of the amplitude of the whirl and SRO as well as phases, however, higher-order SRO was not identified in the experiment.

In the case of active magnetic bearings, the disorder of the sensor signal caused by the runout is misinterpreted as an actual displacement of the rotor, and the AMB generates force to levitate the rotor according to the measured sensor signal including SRO.

Therefore, in order to conduct a more ideal vibration control of the rotation axis, it is necessary to estimate the amplitude and phase of the unbalance and

higher-order SRO. This will enable the rotor to rotate without vibration and lead to a more stable rotation in the high rotation speed.

We have proposed a new identification method for the unbalance and higher-order SRO, and confirmed its effectiveness by a series of simulation [10]. But the convergence speed of the solution is not sufficient for a real-time compensation of mass unbalance.

In this paper, periodic unbalance and higher order SRO are estimated by using an identification method in which the weighted incremental least square on-line method is applied to the experiment.

To improve the accuracy and convergence speed of the solution

(1) The equations of motion of the rotor and the weighted least-square method

The equations of motion of the rotor levitated by AMB are expressed as follows [10].

$$ML\ddot{\hat{x}} + (\omega M_1 L + FK_D)\dot{\hat{x}} + (FK_P + G)\hat{x} + FK_I \int \hat{x} dt = U_1 + ML\dot{x}_r + \omega M_1 L\dot{x}_r + Gx_r \quad (1)$$

where $M, M_1, U_1, F, G, \hat{x}$ are the mass matrix, the gyro-moment matrix, the rotor unbalance matrix, the control stiffness matrix, the negative position stiffness matrix and measured displacement vector at AMB sensor. And K_P, K_I, K_D are the controller gain matrix. The sensor runout vector x_r is represented as follows:

$$x_r = \begin{bmatrix} x_{Ur} \\ y_{Ur} \\ x_{Dr} \\ y_{Dr} \end{bmatrix} = \begin{bmatrix} \sum_{i=1}^n \lambda_{U1} \cos(i\omega t + \phi_{U1}) \\ \sum_{i=1}^n \lambda_{U2} \sin(i\omega t + \phi_{U2}) \\ \sum_{i=1}^n \lambda_{D1} \cos(i\omega t + \phi_{D1}) \\ \sum_{i=1}^n \lambda_{D2} \sin(i\omega t + \phi_{D2}) \end{bmatrix} \quad (2)$$

Taking Laplace transforms of equation (1), we obtain the equation(3) as follows:

$$\left[MLs^2 + (\omega M_1 L + FK_D)s + (FK_P + G) + FK_I \frac{1}{s} \right] \hat{X}(s) = \begin{bmatrix} [H_1(\omega) \cdot s + H_2(\omega)]U_1(s) + [H_3(\omega) \cdot s + H_4(\omega)]U_2(s) \\ + [H_5(\omega) \cdot s + H_6(\omega)]U_3(s) \end{bmatrix} E \quad (3)$$

Substituting equation (4) to equation (3) to take the bilinear z transform of equation(3), we obtain the equation in the z plane as equation (5):

$$s = 2(1 - z^{-1})/T(1 + z^{-1}) \quad (4)$$

$$\Phi(k) = \Omega(k) \cdot E \quad (k = 1 \dots n) \quad (5)$$

In equation (5), the left-hand term $\Phi(k)$ is determined from the dynamic parameters of the rotor and AMB, the sampling period and the measured shaft displacement including the sensor runout and also the $\Omega(k)$ in the right-hand term is determined from the dynamic parameters of the rotor and AMB, the sampling period and the rotating speed. E is an unknown vector, whose elements are unknown static unbalance, dynamic unbalance and high-order SRO and identified by the weighted incremental least-square method.

Dynamic unbalance is angle of center of gravity and principal inertia axis. In this case, principal inertia axis and geometric centerline do not coincide or touch.

As we may use n sets of $\Phi(k), \Omega(k)$ ($k = 1 \dots n$) and get $4n$ equations in equation (6) to identify the unknown vector E

$$\Phi = \Omega \cdot E \quad (6)$$

where

$$\Phi = [\Phi(1) \ \Phi(2) \ \dots \ \Phi(n)]^T \in \mathbb{R}^{4n}$$

$$\Omega = [\Omega(1) \ \Omega(2) \ \dots \ \Omega(n)]^T \in \mathbb{R}^{4n \times 16}$$

In order to minimize the estimation error, the following quadratic cost function J is introduced and E is determined by minimizing the cost function J .

$$J = R^T R = (\Phi - \Omega \hat{E})^T U (\Phi - \Omega \hat{E}) \quad (7)$$

where $R = \Phi - \hat{\Phi} = \Phi - \Omega \hat{E}$ is the estimation error. U is weighted matrix, and $\hat{\Phi}$ is identification value of Φ . Its minimum satisfies

$$\frac{\partial J}{\partial E} = -2\Omega^T U \Phi + 2\Omega^T U \Omega \hat{E} = 0 \quad (8)$$

Then, equation (9) is obtained.

$$\Omega^T U \Phi = \Omega^T U \Omega \hat{E} \quad (9)$$

If $\Omega^T \Omega$ is the non-singular matrix, \hat{E} , the identified value of E , is derived from the above equation.

$$\hat{E} = (\Omega^T U \Omega)^{-1} \Omega^T U \Phi = P_n b_n \in \mathbb{R}^{16} \quad (10)$$

(2) Applied incremental on-line algorithm

The incremental on-line method is a method to improve the latest estimated value, whenever new data are obtained. In this study, identification of the unbalance and SRO is conducted with the incremental on-line method. By using this method the unknown vector E can be identified in real-time without the necessity to save data.

Now, the identified value obtained from k -th measured data is represented by $\hat{E}(k)$, and $\hat{E}(k)$ is identified by using $\hat{E}(k-1)$. The incremental least

square on-line method [10] is represented by the following algorithm.

$$P_n = (\Omega_n^T U \Omega_n)^{-1} \in R^{16 \times 16} \quad (11)$$

$$P_n^{-1} = P_{n-1}^{-1} + \Omega^T(n) U \Omega(n) \quad (12)$$

Multiplying equation (7) by P_n on the left and by P_{n-1} on the right, we can get the following equation:

$$P_{n-1} = P_n + P_n \Omega^T(n) U \Omega(n) P_{n-1} \quad (13)$$

and find the inverse matrix of equation (7)

$$P_n = P_{n-1} - P_{n-1} \Omega^T(n) (U^{-1} + \Omega(n) P_{n-1} \Omega^T(n))^{-1} \Omega(n) P_{n-1} \quad (14)$$

multiplying equation (8) by $\Omega^T(n) [U^{-1} + \Omega(n) P_{n-1} \Omega^T(n)]^{-1} \Omega(n) P_{n-1}$ produces the following equation:

$$\begin{aligned} P_{n-1} & \left[\Omega^T(n) (U^{-1} + \Omega(n) P_{n-1} \Omega^T(n))^{-1} \Omega(n) P_{n-1} \right] \\ & = P_{n-1} \Omega^T(n) (U^{-1} + \Omega(n) P_{n-1} \Omega^T(n))^{-1} \Omega(n) P_{n-1} \\ & = P_{n-1} - P_n \\ & = P_n \Omega^T(n) U \Omega(n) P_{n-1} \end{aligned} \quad (15)$$

Equation (11) is derived from equation (9) and (10).

$$P_n \Omega^T(n) U = P_{n-1} \Omega^T(n) (U^{-1} + \Omega(n) P_{n-1} \Omega^T(n))^{-1} \quad (16)$$

n -th identified vector \hat{E}_n is obtained from equation (11) as follows:

$$\begin{aligned} \hat{E}_n & = P_n b_n \\ & = [P_{n-1} - P_{n-1} \Omega^T(n) (U^{-1} + \Omega(n) P_{n-1} \Omega^T(n))^{-1} \Omega(n) P_{n-1}] \\ & \quad \times [b_{n-1} + \Omega^T(n) U \Phi(n)] \\ & = E_{n-1} - P_{n-1} \Omega^T(n) (U^{-1} + \Omega(n) P_{n-1} \Omega^T(n))^{-1} \Omega(n) E_{n-1} \\ & \quad + P_n \Omega^T(n) U \Phi(n) \\ & = E_{n-1} - P_n \Omega^T(n) U \Omega(n) E_{n-1} + P_n \Omega^T(n) U \Phi(n) \\ & = E_{n-1} - P_n \Omega^T(n) U [\Omega(n) E_{n-1} - \Phi(n)] \end{aligned} \quad (17)$$

Then, the unbalance and runout are calculated from the estimated \hat{E} .

Experiments

(1) Experimental apparatus

Figure 1 shows the experimental apparatus for evaluating the proposed identification method of the mass unbalance and SRO. The apparatus uses an overhung rotor of turbo molecular vacuum pump. The rotor is supported by two AMB, namely upper AMB

and lower AMB. The AMB have two proximity sensors in orthogonal directions x-y to measure and regulate the relative displacements between the rotor and the stator. The AMB analog controllers consist of sensor boards, PID controllers and PWM power amplifiers. The output from the sensor boards, which are proportional to the relative displacements, are connected to the A/D converters in DSP board which is a 32 bit floating point machine using a Texas Instruments TMS320C30 digital signal processor.

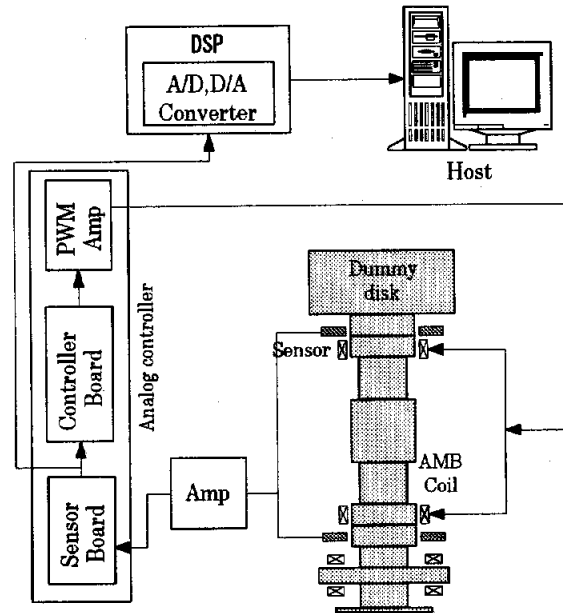


Fig. 1 Apparatus of Turbo Molecular Pump

The rotor is 204.3mm in length, 2.59kg in total mass, 11442.23 kgmm² in radial moment of inertia, and 1785.05 kgmm² in polar moment of inertia and has a dummy disk on the top to install a known unbalance to evaluate the accuracy of the identification method.

After measuring the rotation speed at two specified rotations, the analog vibration data are converted to digital signals at the constant sampling frequency. At this time the sampling cycle is 600 microseconds and the number of data is 5000 (3 seconds).

A pair of identification tests are carried out to verify the accuracy of the method. Firstly, the unbalance and SRO are identified without an attached unbalance. After that, a known unbalance weight is attached on the dummy disk and a second identification test is carried out.

(2) The comparison of the weighted least-square method and least-square method

The conventional incremental least-square method is

a linear identification method. However, as the measured whirling data includes observation error, the convergence has been improved by using the weighted incremental least-square on-line method. The rotating speeds were set at 500 rpm and 1500 rpm. Measured shaft vibration data are shown in figure 6. The identified static unbalance (ϵ), dynamic unbalance (τ), and SRO are shown in figure 2 - 5. The left side figures and the right side figures show the amplitude and the phase angles of the unbalance and the sensor runout respectively. Thick solid lines indicate the result of the weighted least-square method, thin solid lines indicate the result of the conventional least-square method and dot-dash lines are calculated values by using the vector diagram. The experiments of the weighted least-square method, just after a change of the rotating speed from 500rpm to 1500rpm, static unbalance (ϵ), dynamic unbalance (τ) amplitude and phase angles of the identified parameters converge to the calculated values rapidly. Also, the 1st component of SRO converge to the constant values. But for the static unbalance (ϵ), the dynamic unbalance (τ) and 1st component of SRO, it takes more than 2 seconds to converge. since the 2nd and 3rd component of SRO are small, no remarkable change in convergence is observed.

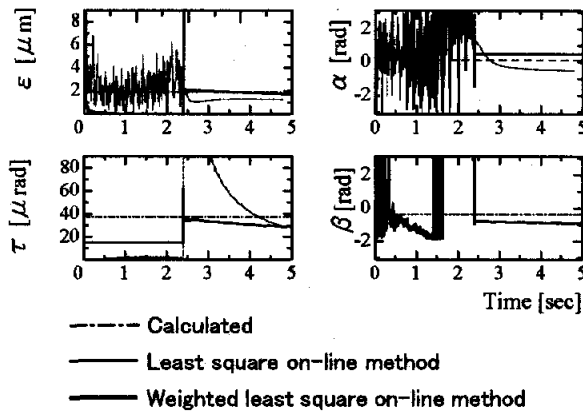


Fig.2 Estimated Unbalance and phase using measured data

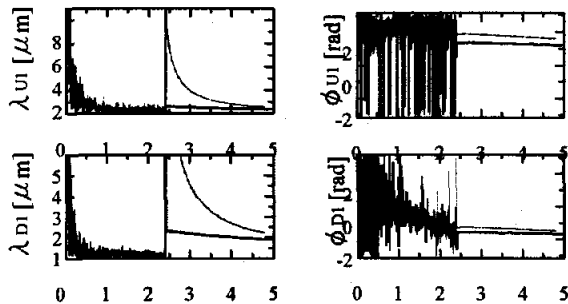


Fig.3 Estimated 1st order SRO and phase using measured data

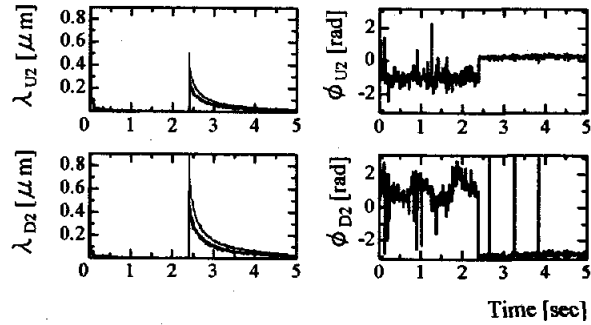


Fig.4 Estimated 2nd order SRO and phase using measured data

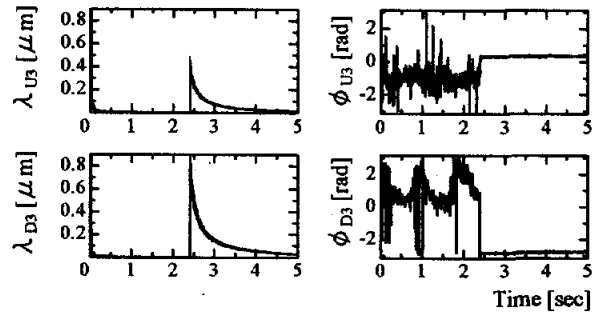


Fig.5 Estimated 3rd order SRO and phase using measured data

(3) Experimental identification

The synchronous unbalance and high-order SRO are identified by obtaining the shaft vibration data when a weight is not attached to the rotor and when weights of 0.1g (Exp I) and 0.5g (Exp II) are attached to the rotor at phase angle 0° from the key phaser of the rotor supported by active magnetic bearing. The rotating speeds were set at 500 rpm and 1500 rpm. The shaft vibration data are shown in figure 6 and figure 7. Figures 8-11 show the identification process of mass unbalance, 1st, 2nd, and 3rd component of SRO respectively. Thick dot-dash lines indicate the result of calculated values by using the vector diagram with unbalance mass 0.5g, thick solid lines indicate the result of unbalance mass 0.5g, thin dot-dash lines indicate the result of calculated values by unbalance mass 0.1g, thin solid lines indicate the result of unbalance mass 0.1g, and thin dot lines indicate the result of residual unbalance.

The identified result of Exp. I and Exp. II are shown in Tables 1 and 2. Where each of the experiment results compared with the calculated value by using the vector diagram. Figure 8 shows the difference of about 15%-24% between the identified value and calculated value of the static unbalance (ϵ) and dynamic unbalance (τ). Also, when a light weight (0.1g) is attached, the difference between the calculated value

and identified value of static unbalance phase (α) and dynamic unbalance phase (τ) is 30° . When a heavy weight (0.5g) is attached, an angular error is 15° . The SRO of the surface of the rotor's upper and lower AMB is shown in figures 5, 6, and 7 as λ_{Ui} , λ_{Di} , ($i=1,2,3$) and the phase is expressed as ϕ_{Ui} , and ϕ_{Di} ($i=1,2,3$). The identified result is indicated to the 3rd order. As in the diagram, the identification results when numerous weights are attached and when a weight is not attached to the rotor almost correspond. The phase is converged into a constant value, though there is error respectively.

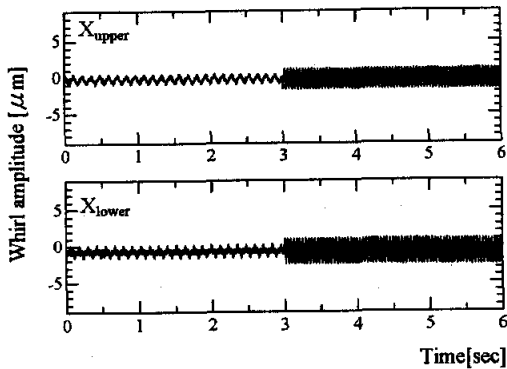


Fig.6 shaft vibration with added trial mass 0.1g

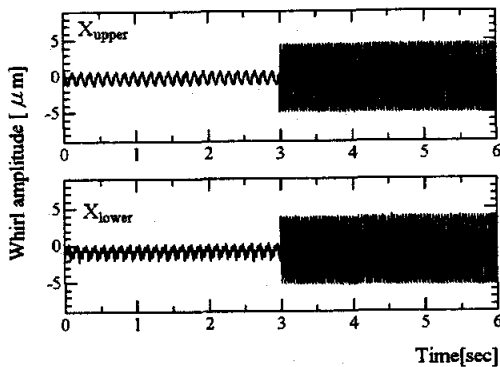


Fig.7 shaft vibration with added trial mass 0.5g

Table 1 Identification results of unbalance

Mass	Trial weight (0.1g)			
	Experiment	Exp. I	Cal.	Error
Unbalance	Static(μm)	1.78	1.88	5%
	Dynamic(μrad)	29.5	37.3	20%
Phase	Static (rad)	0.49	0.1	0.39
	Dynamic (rad)	-0.9	-0.38	0.52

Table 2 Identification results of unbalance

Mass	Trial weight (0.5g)			
	Experiment	Exp. II	Cal.	Error
Unbalance	Static(μm)	7.55	9.87	23.5%
	Dynamic(μrad)	135.0	163.1	17%
Phase	Static (rad)	-0.13	0.02	0.15
	Dynamic (rad)	-0.35	-0.08	0.27

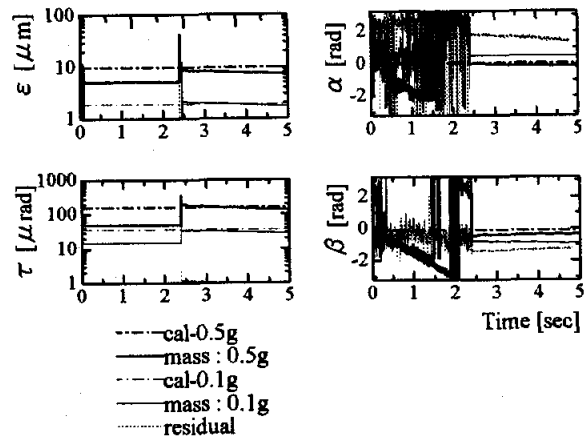


Fig.8 Unbalance and phase from experiment

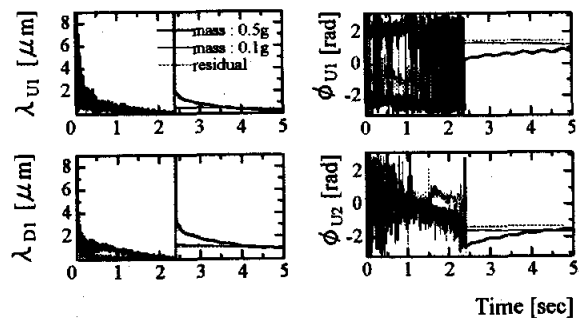


Fig.9 1st component of SRO and phase from experiment

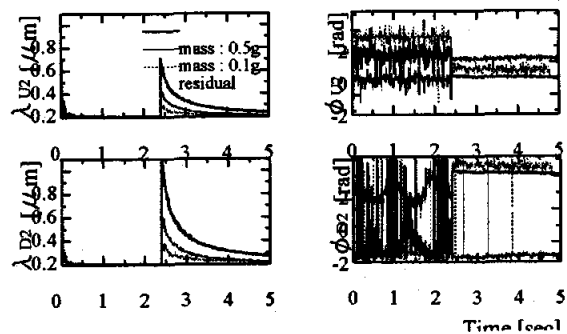


Fig.10 2nd component of SRO and phase from experiment

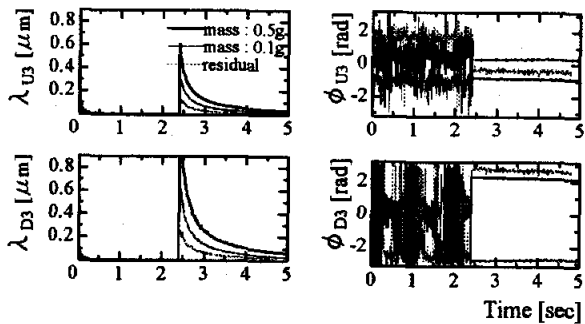


Fig.11 3rd component of SRO and phase from experiment

Conclusions

We identified the mass unbalance and SRO on the rotor supported by AMB using the incremental least square method and weighted incremental least square method and were led to the following conclusions:

1. It becomes clear that the synchronous mass unbalance and higher-order SRO are identified by the weighted incremental least square on-line method or the conventional incremental least square method using the measured shaft vibration data of the turbo molecular pump rotor supported AMB and
2. The weighted incremental least square on-line method has faster convergence speed of the solution than the conventional incremental least square method.
3. The identified values of the 1st component of SRO and phase with a trial added mass corresponds with the identified values before adding the trial mass. The 2nd and 3rd component of SRO were correctly estimated. However, discrepancies of their phase were about 30° between the identification with and without the trial mass.

References

1. Matumura F., Fujita M. and Tsukamoto M., Digital control system for magnetic bearings with automatic balancing. Proc. of the 2th int. Symp. on Magnetic Bearings, pp.12-14, 1990.
2. Kim, C.-S., Lee, C.-W., In Situ Runout Identification in AMB System by Extended Influence Coefficient Method, IEEE/ASME trans. On Mechatronics, vol.2, no.1, pp.51-57, 1997.
3. Carl R. Knope, R.W. Hope, S.J. Fedigan, and R.D. Williams, Experiments in the control of

unbalance response using magnetic bearings, *Mechatronics*, vol.5, no.5, pp.385-400, 1995.

4. B. Shafai, S. Beale, P. LaRocca, and E. Cusson, Magnetic Bearing Control Systems and Adaptive Forces Balancing, IEEE Control Systems, vol.14, pp.4-13, April 1994.
5. Mizuno, T., Higuchi, T., Design of Magnetic Bearing Controllers Based on Disturbance Estimation, Proc. of the 2th int. Symp. on Magnetic Bearings, pp.281-288, 1990.
6. J.D. Setiawan, R. Mukherjee, E.H. Maslen, Adaptive compensation of sensor runout for magnetic bearings with uncertain parameters: Theory and experiments, ASME J. Dyn. Syst. Meas., vol.123, pp.211-218, Jun 2001.
7. Liu ZH, Nonami K, Adaptive vibration control using frequency estimation for multiple periodic disturbances with noise, JSME, SERIES C, vol.43 (3), pp 719-725 Sep 2000.
8. A.R. Boletis, A. Schammas, F. Barrot, H. Bleuler, Study of Repetitive and Non Repetitive Runout for High Precision Rotating Machines on Active Magnetic Bearings, Proc. of the 5th int. Symp. on Magnetic Bearings, pp.48-52, 1996.
9. J.D. Setiawan, R. Mukherjee, E.H. Maslen, Variable Magnetic Stiffness Approach for Simultaneous sensor runout and Mass Unbalance Compensation in Active Magnetic Bearings, Proc. of the 7th int. Symp. on Magnetic Bearings, pp.549-554, Aug. 2000.
10. Kanemitsu, Y., Kijimoto, S., and Matsuda, K., Park, T.-J., Identification of Mass Unbalance and Sensor Runout on a Rotor Equipped with Magnetic Bearings, Proc. of the 7th int. Symp. on Magnetic Bearings, pp.543-548, 2000.